Temperature Dependent Electron Binding in $(H_2O)_8$

Marcelo A. Carignano,* Anis Mohammad, and Sabre Kais

Department of Chemistry, Purdue University, West Lafayette, Indiana 47907

Received: February 04, 2009; Revised Manuscript Received: June 22, 2009

We combine classical molecular dynamics simulations and quantum density functional theory calculations to study the temperature effects on the electron affinity of the water octamer. The atomistic simulations provide a sample of the cluster's conformations as a function of the temperature, on which the density functional calculations are carried on. As the temperature increases, the cluster undergoes its characteristic phase change from a cubic, solidlike structure to a liquidlike state. This phase change is also reflected by an increase on the total dipole moment of the cluster. The quantum calculations indicate that the large dipole moment conformations have a positive electron affinity. Relaxing the high temperature conformations of the cluster anion to its local minimum, the average vertical detachment energy is calculated and shows a clear tendency to increase as the temperature increases. The analysis of the high temperatures conformations reveals that origin of higher values of the vertical detachment energy is not the stability of the negative octamer but the high energy of the corresponding neutral cluster.

I. Introduction

Since the first observation of negatively charged water clusters in 1981,[1] the interest on water clusters and their ability to bind an excess electron has never declined.[2−13] Clusters have the advantage that they are more accessible to exhaustive computational studies than bulk systems, and therefore many theoretical works are dedicated to them. Theoretical results combined with spectroscopic techniques allowed the characterization of water cluster anions according to their vertical detachment energy (VDE).[9,8,14−16] These isomeric types are labeled I, II, and III in order of decreasing VDE. Water cluster anions are also interesting because they are expected to contribute to the understanding of the hydrated electron, which plays a significant role in radiation induced processes, biological reactivity, atmospheric chemistry in water droplets, and charge induced reactivity.

In their pioneer work, Armbruster et al.[1] created water cluster anions by injecting electrons from a radioactive foil into a condensation chamber with warm water vapor, which is then supersonically expanded through a nozzle. The authors claim that eight water molecules are sufficient to capture an excess electron. Subsequent experiments performed Haberland et al.[3,4] with a similar approach, but using low energy electrons of less than 1 eV, failed to observe the octamer anion. With Xe as carrier gas, the octamer anion is observed, but it is missing if the carrier gas is Ar. Knapp et al.[5] were able to attach an electron to existing cold neutral water clusters with at least 11 molecules. Their technique requires the use of cold electrons, with energy close to 0 eV. In conclusion, the early experiments are somewhat contradictory with respect to the existence of a stable $(H_2O)_8^-$. In their discussion, Kanpp et al.[5] speculate on the role of temperature on this particular cluster size and state that hot octamers may be able to trap low energy electrons.

The water octamer represents a very interesting case since its lowest energy structures, the D2d or S4 cubic conformations,[17,18] have zero total dipole moment and no electron binding is possible. As the temperature increases, the cluster undergoes a phase change[17,19] and is free to adopt conformations of finite total dipole moment that favor the binding of an electron. An ideal dipole will bind an electron if the dipole moment is larger than the critical value $\mu_c = 1.6648$ D.[20] However, subsequent experimental and computational studies taking into account corrections to the Born−Oppenheimer approximation give the more realistic estimate of $\mu_c = 2.5$ D.[2,21] Upon the binding of an electron, the system's potential energy surface changes, and this change may induce a conformational evolution to a different state that may or may not be energetically favorable for the cluster anion. In consequence, the electron may remain bound to the cluster or be released.

A recent ab initio study by Lee and Kim[22] has addressed the structure and electronic properties of $(H_2O)_8^-$. They have found that the most stable structures of the anion are cubic, as is the case for the neutral cluster, but with a different arrangement of hydrogen bonds. All the cubic structures for the water octamer have four "daa"-type (donor−acceptor−acceptor) molecules, and four "dda"-type (donor−donor−acceptor) molecules. It is the relative position of these molecules that most affects the binding of an extra electron. Namely, the ability of the cluster to bind an extra electron is affected by the position of the dangling hydrogen atoms. According to ref 22, the lowest energy system (Cdh) has the electron bound to a central dangling H atom, on a structure characterized by having the dangling H atoms sharing three edges of the cubic cluster and converging to a central dangling H atom. Two other low energy conformers were found (Cd and Cd″) with the four dangling H atoms on the face of the cube. The VDE energies calculated using MP2/aug-cc-pVDZ+(2sp/s) are larger for Cd and Cd″ conformers (0.40 and 0.38 eV) than for the Cdh lowest energy structure (0.25 eV). Another structure (Cb) having yet higher energy, and involving 11 hydrogen bonds to form a deformed cube leaving one "aa"-type molecule to bind the electron with an even higher VDE (0.73 eV). Isomer-specific spectroscopy experiments by Roscioli and Johnson[23] reveal that the type I isomers of $(H_2O)_8^-$ are consistent with the red-shift signature of an "aa"-type molecule, while the type II isomers show a red shift consistent with the electron bound to a single dangling hydrogen.

* Corresponding author. E-mail: cari@purdue.edu.

10.1021/jp901047y CCC: $40.75
Published on Web 09/01/2009

In this Article we combine classical molecular dynamics (MD) simulations and density functional theory (DFT) calculation to study the vertical detachment energy for $(H_2O)_8^-$ as a function of temperature. The MD simulations are used to calculate the temperature dependency of the neutral cluster dipole moment and to generate typical cluster conformations for the temperature range 5−235 K. Using these conformations as a starting point, DFT calculations are carried out to determine the dipole moment of the neutral cluster from the electronic density, the instantaneous binding energy (iBE) and the vertical detachment energy (VDE). In the following section we describe the calculation details and the results are presented and analyzed in section III.

II. Calculation Details

Molecular dynamics simulations were performed using GROMACS v3.3.3.[24−26] The water molecules were described using the SPC/E model.[27] The water octamer was placed in a cubic simulation box, with an edge size of 2.1 nm. All the interaction were cut off at 1.0 nm, a distance larger than the largest separation between any atom pair in the cluster at any temperature. The simulations used a time step of 0.001 ps and were done under constant NVT conditions. These settings ensure that the interactions within the cluster were fully accounted for and no influence of the periodic images may occur.

The temperature effects on the water octamer was studied using the replica exchange technique,[28] in which several simulations at different temperatures are performed simultaneously. We have considered 24 different temperatures from 5 to 235 K in steps of 10 K, attempting an exchange between the conformations of neighboring temperatures every 10 ps (10 000 steps). This conformation exchange facilitates the system to overcome energy barriers avoiding the trapping of the cluster in a particular valley of the energy landscape. The exchange between conformation a and b corresponding to temperature T_a and T_b is accepted with a probability

$$P_{ab} = \min\left(1, \exp\left[\frac{1}{k_B T_a} - \frac{1}{k_B T_b}\right](U_a - U_b)\right) \qquad (1)$$

where k_B is the Boltzmann constant and U_i is the total potential energy of conformation i at the time when the exchange is attempted. The total simulation time was 10 ns (10^7 steps), and the rigid water architecture was maintained during the simulation using the SHAKE algorithm.[29]

From the trajectories obtained with the molecular dynamics simulations we extract a sample of cluster conformations by saving the cluster coordinates every 1 ns of simulation for each temperature. These conformations are subsequently used as input coordinates to perform density functional (DFT) theory calculations using the Gaussian-03 (rev D1) program suite.[30] All the quantum calculations were performed using the B3LYP functional in combination with the aug-cc-pVDZ basis set. This functional/basis set combination was chosen as a compromise between accuracy and computational time.

On most of the selected conformations, we perform four DFT calculations. First, we perform a single point calculation of the electrically neutral cluster (E_0) and the corresponding negative ion (E_0^-). These results will determine the instantaneous electron binding energy as iBE = $E_0 - E_0^-$. This is done for each conformation from the sample. A positive iBE indicates that the cluster energetically favors the attachment of an extra electron.

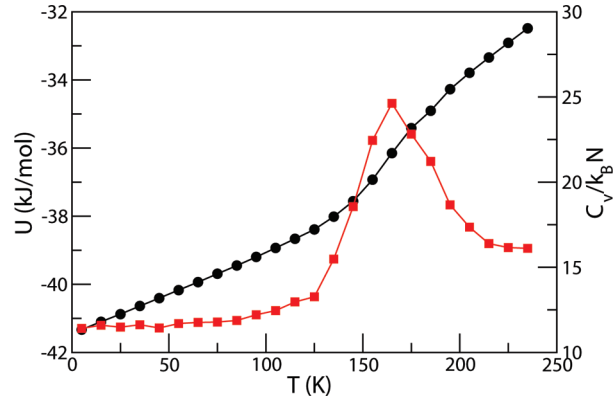

Figure 1. Potential energy (U, black circles) and the heat capacity (C_v, red squares) of the neutral water octamer as a function of the temperature calculated from MD simulations using SPC/E model.

Then, for the high temperature conformations, we perform an optimization of the negatively charged clusters (E_1^-) followed by another single point calculation on the same optimized structure (E_1) but with zero charge. These steps are to determine the vertical detachment energy, VDE = $E_1 - E_1^-$.

The results that follow are presented with three different energy units. We made this choice due to the nature of the previous results from different calculation schemes or experiments with different customary units. For example, in atomistic computer simulations the potential energy is usually expressed in kJ/mol, and therefore we used that unit to present our MD results. Quantum calculations are commonly presented in atomic units, and the experimentally accessible vertical detachment energies are reported in eV.

III. Results and Discussion

For low temperatures, the octamer has a cubiclike structure, which became increasingly distorted as the temperature approaches the transition temperature T_m. At temperatures higher than the T_m, the cluster undergoes continuous structural transformations in line with a liquidlike state. The cluster potential energy, obtained from the MD simulations, is displayed in Figure 1 along with the heat capacity C_v that shows a peak at T_m. For the SPC/E model, the transition temperature is T_m = 165 K. This phase change has been extensively studied with atomistic simulations, and it is clear that the transition temperature is dependent on the molecular model used to describe the intermolecular interactions.[31−33] A more accurate description of the water octamer phase change would be possible using more sophisticated models including, for example, atomic polarizabilities[34] and/or extended charge distributions.[35] However, this would not affect the general conclusions of the present work, which aims to understand in general terms the role of temperature on the ability of a water octamer to bind an electron.

In Figure 2, we show the average cluster binding energy calculated using the sample of conformations taken from the MD simulations. The binding energy was calculated by direct difference of the cluster total DFT energy minus 8 times the energy of the isolated water molecule in its optimal conformation. Comparing the DFT and MD energy curves, we note that they have qualitatively the same temperature dependency, although the SPC/E curve is more negative by approximately 11 kJ/mol. This is not surprising, since the SPC/E model considerably overestimates the dimer binding energy. From the same DFT calculation we obtain the average cluster dipole moment, which compares remarkably well with the results from

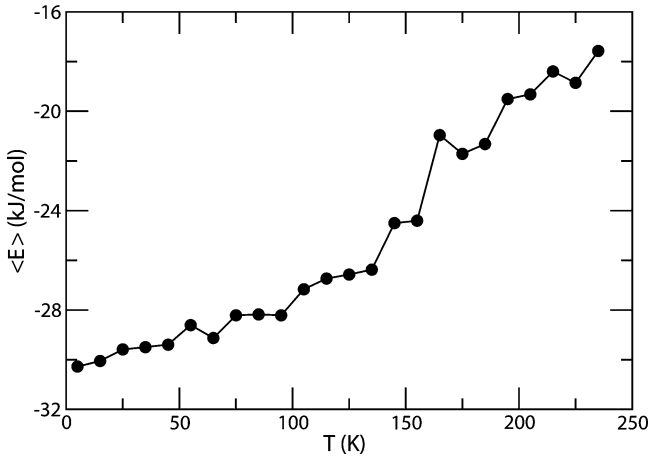

Figure 2. Average binding energy of $(H_2O)_8$ calculated from a sampling of conformations from the MD simulations, using density functional theory.

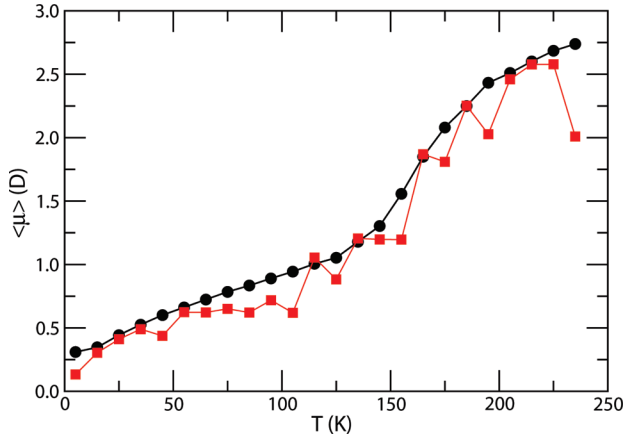

Figure 3. Average dipole moment from MD simulations (black circles) and from density functional theory (red squares) as a function of temperature.

the MD simulations, as shown in Figure 3. The cluster dipole moment increases with the temperature, following a trend similar to the cluster binding energy. This increase in the dipole moment suggests that the cluster may be able to bind an extra electron for sufficiently high temperatures.

When the neutral clusters are exposed to cold electrons, as in the experiment of Knapp et al.,[5] an electron may be trapped by the cluster only if the instantaneous cluster conformation favors the binding. To evaluate this possibility, we performed DFT calculations on anionic clusters of the sample conformations taken from the MD simulations. If the energy of the anion (E_0^-) is smaller than the energy of the equivalent neutral cluster (E_0), then we conclude that this particular conformation will trap an extra electron. The average of the instantaneous binding energy, $\langle \text{iBE} \rangle = \langle E_0 - E_0^- \rangle$, is a measure of the likelihood of the electron binding. In Figure 4 we show the ⟨iBE⟩ as a function of temperature. Interestingly, the ⟨iBE⟩ increases with temperature and becomes positive for temperature just below T_m. For temperatures lower than T_m, where the cluster has a closed cubic conformation, there is no possibility of electron binding, but for higher temperatures, as the cluster starts to break some of the internal hydrogen bonds to explore open conformations, the attachment of an extra electron is possible.

Once an electron has been attached to an initially neutral cluster, the energy landscape of the system changes and it is reasonable to expect a time evolution of the cluster geometry

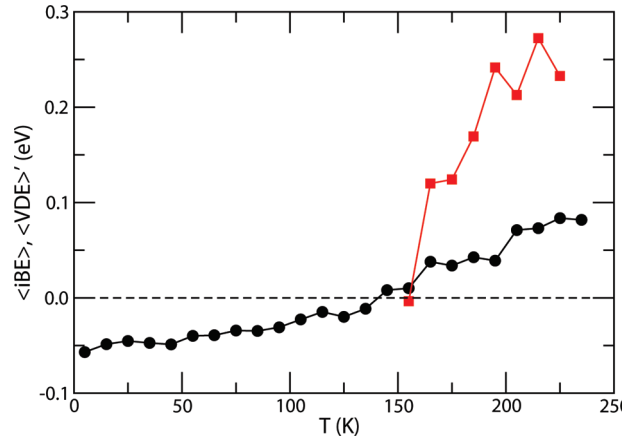

Figure 4. ⟨iBE⟩ (black circles) and ⟨VDE⟩′ (red squares) obtained from averaging the energy results from density functional theory on the sample conformations obtained in the MD simulations.

different from that of the neutral cluster. In other words, the energy valley in which the cluster resides may change in several different ways. For example, the extra electron may decrease (or increase) the floor of the energy landscape, so that the cluster may now relax to a more (less) stable conformation, or it may lower or remove some energy barriers so that the cluster will adopt a different structure. Let us consider that the cluster will relax and eventually reach its new local minima; then we can calculate the vertical detachment energy for the newly optimized cluster anion. Some of the optimized anions are more stable than the neutral clusters, but some of them are not. We defined ⟨VDE⟩ considering only the stable negative clusters, but we also calculate the average ⟨VDE⟩′ (≤⟨VDE⟩) that includes all the conformations. In Figure 4 we show that ⟨VDE⟩′ increases with temperature from a small negative number for $T = 155$ K up to ∼0.25 eV for $T = 225$ K. For $T = 235$ K the optimization of the negative cluster leads in several cases to separation of the cluster in fragments, so we have excluded this temperature from the analysis. Except for $T = 155$ K, where most of the sample structures relax to a nonbinding cubic structure, we find the ⟨VDE⟩′ > ⟨iBE⟩. This indicates that, on average, once an electron is captured, the relaxation of the cluster will lead to a stable water anion.

The averages ⟨VDE⟩ and ⟨VDE⟩′, along with the minimum and maximum values in the sample are plotted in Figure 5. For each temperature except 215 K, there is at least one structure that relaxes to an unstable conformation for $(H_2O)_8^-$. We find no special reason for 215 K to not find a conformation that will relax to a similar low energy structure as for the other temperatures, except in our limited statistical sample. The structure corresponding to this non electron binding cluster is cubic, with the extra electron orbital being split among several dangling hydrogen atoms. This is clearly displayed by the isosurfaces of the corresponding HOMO, shown below in Figure 7A. The curve corresponding to the maximum VDE reaches values in line with type I isomers (see Figure 1 of ref 16). Other structures relax to energies consistent with type II and type III isomers. Therefore, depending on the instantaneous conformation of the neutral cluster when the extra electron is first attached, the subsequent relaxation will take the cluster to a different isomeric form that may be of any of the three types commonly used to classify them. Moreover, the relaxed structure may not favor the electron binding at all.

To analyze the origin of the high VDE values, we plot in Figure 6 the VDE corresponding to all the structures in the MD

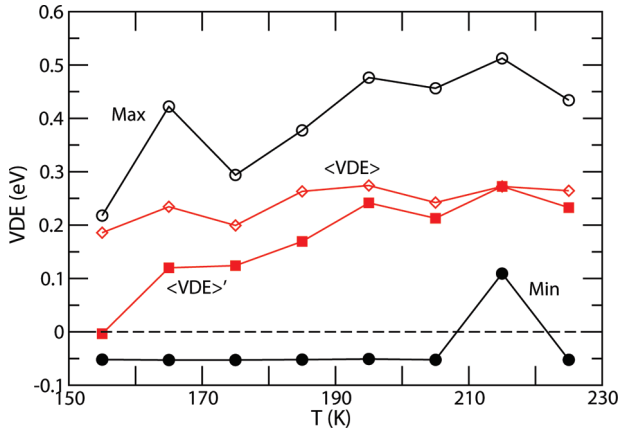

Figure 5. ⟨VDE⟩ (open red diamonds) and ⟨VDE⟩′ (filled red squares), maximum (open black circles), and minimum (filled black circles) values of the VDE from the sample conformations as function of temperature.

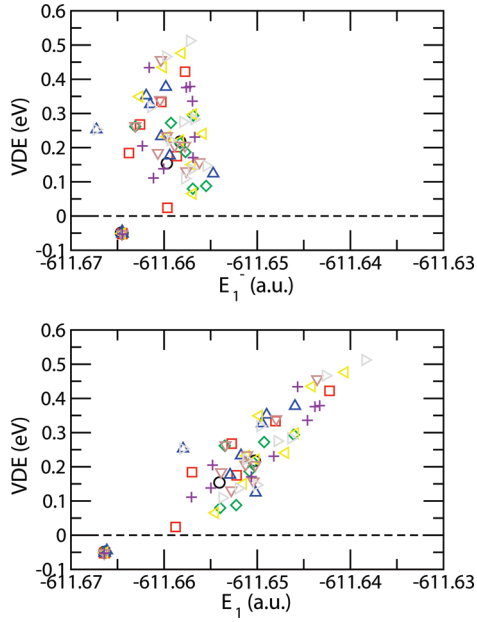

Figure 6. Vertical detachment energy from density functional calculations as a function of the energy of the optimized anion (top panel) and the energy of the corresponding neutral cluster (bottom panel). The different colored symbols are for different temperatures: black (155 K), red (165 K), green (175 K), blue (185 K), yellow (195 K), brown (205 K), gray (215 K), and violet (225 K).

sample, as a function of both the energy of the optimized anion E_1^- (top panel) and the energy of the corresponding neutral cluster E_1 (bottom panel). E_1^- takes values over a narrow range of 0.01 au to around −611.66 au. On the other hand, E_1 has a more extended range, and more interestingly, the VDE seems to have a linear relationship with E_1. The conclusion is that large VDE values are mainly due to the large instability (large E_1) of some neutral cluster that became locally stabilized when attaching an extra electron. As an example, we show in Figure 7B the structure of the case of highest VDE (gray triangle in Figure 6, VDE ∼ 0.5 eV, E_1^- = −611.657 au). The HOMO orbital isosurface shows the electron bound to four H atoms, and the structure could be described as a tetramer and a pentamer sharing one water molecule. The extra electron stabilizes the structure. The high energy of the neutral cluster (and consequently the large VDE) is immediately apparent from the structure that has only 9 hydrogen bonds out of a possible total of 12.

The most frequent cubic structure obtained in this work correspond to the D2d and S4 geometries, one of which is shown in Figure 7A. These two isomers have nearly the same energy (E_1^- = −611.666 au, VDE = −0.05 eV). Two of the cubic structures reported in ref 22 and labeled Cd and Cd″, which have the four dangling H atoms on the same face of the cube, have not been found in this study.

The optimal structure (E_1^- = −611.667 au, VDE = 0.25 eV) from our sample, which we will label Cc, is displayed in Figure 7C and has three dangling H atoms on one of the cubic faces. This structure is different from the Cdh of ref 22, which has not been observed. Our Cc cluster is similar, but not exactly the same, as the E8 structure of ref 18. Even though this structure has the lowest total energy of the whole sample, the VDE values correspond to type II isomers due to the low energy of its neutral counterpart. Another interesting structure is displayed in Figure 7D (E_1^- = −611.660 au, VDE = 0.44 eV). This cluster has only 9 hydrogen bonds and consists of two pentamer rings connected by a shared side. The two rings are folded so that they form an angle of approximately 90°, leaving space for the extra electron to bind to four dangling H atoms.

There are two important factors that have a strong influence on the cluster energy and its vertical detachment energy. First, the overall symmetry of the structure that we can characterize by the total number of hydrogen bonds, and second, the organization of the dangling H atoms that create an adequate pocket for the extra electron to bind. Having more hydrogen bonds will result in a low energy cluster, regardless of the presence of the extra electron. Having more dangling H atoms on a small region will also result in a low energy cluster anion, but the corresponding neutral cluster will pay an energy penalty. The VDE results from the interplay of these two effects.

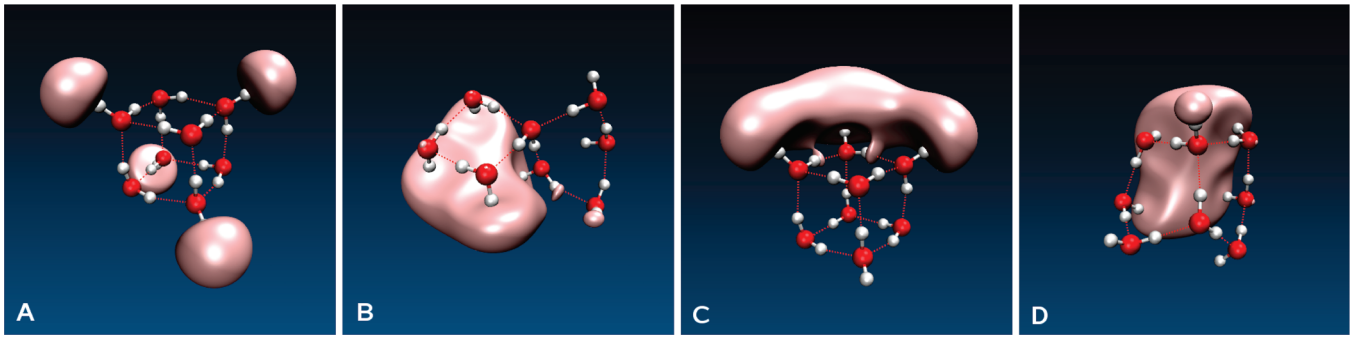

Figure 7. Structure and isosurface of the HOMO orbital (value 0.02) for (A) a nonbinding S4 structure, (B) the cluster corresponding to the maximum VDE (0.51 eV), (C) the lowest energy structure (Cc) obtained from minimizing the cluster anions from initial position taken from the MD sampling, and (D) a typical structure stabilized by an extra electron, which becomes unstable if the electron is removed.

IV. Discussion

The use of density functional theory for the calculation of VDEs was recently questioned by Herbert and Head-Gordon,[36] in particular for small clusters. They performed a detailed study of the VDEs for various conformers of $(H_2O)_n$ using both DFT and wave function methods in sequences of increasingly diffuse Gaussian basis sets. For $n \leq 6$, MP2 and CCSD(T) results for the VDE converge to within ~0.01 eV of the complete basis-set limit using highly diffuse Pople-style basis sets. MP2 perturbation theory produces results for the VDE that are consistently below the coupled-cluster value for the same basis set. On the other hand, it was found that DFT functionals lead to a significant overbinding as compared with the best theoretical estimates and experimental values. Interestingly, the Becke "half and half" functional gives results for the VDE only ~30 meV higher than the CCSD(T) values. A similar study is not available for clusters with eight water molecules and is difficult to assess the quantitative accuracy of the results presented here. However, our results show a logical physical picture consistent with experimental observations. Moreover, the values for the VDEs were found to be in the range of energies, supporting the conclusion that many different conformers are formed, as is also clearly shown in the compilation presented in Figure 1 of ref 16.

In conclusion, by combining classical MD simulations with DFT calculation we provide a different, complementary approach to study water clusters and their ability to attach an extra electron. The water octamer, having zero dipole moment in its optimal structure, is able to bind an electron only at temperatures around or above the cluster melting temperature, which we estimate at 165 K for the SPC/E model. The higher the temperature is, the more likely the cluster will explore conformations that will instantaneously favor electron binding. Also, the relaxation of the cluster once ionized results in a temperature dependency of the average VDE, which increases with temperature. Yet, at every temperature there are conformations that will initially bind an electron, but the subsequent relaxation will lead the cluster to a cubic conformation of low (or null) dipole moment and the electron will then be released. On the other hand, the conformations with the highest VDE are characterized by open structures, which are held together by the extra electron and will be highly unstable if the electron is suddenly removed.

References and Notes

(1) Armbruster, M.; Haberland, H.; Schindler., H.-G. *Phys. Rev. Lett.* **1981**, *47*, 323–326.
(2) Simons, J. *J. Phys. Chem. A* **2008**, *112*, 6401–6511.
(3) Haberland, H.; Langosch, H.; Schindler, H. G.; Worsnop, D. R. *J. Phys. Chem.* **1984**, *88*, 3903–3904.
(4) Haberland, H.; Ludewigt, C.; Schindler, H.-G.; Worsnop, D. R. *J. Chem. Phys.* **1984**, *81*, 3742–3744.
(5) Knapp, M.; Echt, O.; Kresle, D.; Recknagel, E. *J. Phys. Chem.* **1987**, *91*, 2598–2601.
(6) Campagnola, P. J.; Cyr, D. M.; Johnson, M. A. *Chem. Phys. Lett.* **1991**, *181*, 206–212.
(7) Arnold, S. T.; Morris, R. A.; Viggiano, A. A. *J. Chem. Phys.* **1995**, *103*, 9242–9248.
(8) Kim, J.; Becker, I.; Cheshnovsky, O.; Johnson, M. A. *Chem. Phys. Lett.* **1998**, *297*, 90–96.
(9) Coe, J. V.; Lee, G. H.; Eaton, J. G.; Arnold, S. T.; Sarkas, H. W.; Bowen, K. H.; Ludewigt, C.; Haberland, H.; Worsnop, D. R. *J. Chem. Phys.* **1990**, *92*, 3980–3982.
(10) Desfrancois, C.; Khelifa, N.; Lisfi, A.; Schermann, J. P.; Eaton, J. G.; Bowen, K. H. *J. Chem. Phys.* **1991**, *95*, 7760–7762.
(11) Ayotte, P.; Johnson, M. A. *J. Chem. Phys.* **1997**, *106*, 811–814.
(12) Hammer, N. I.; Shin, J.-W.; Headrick, J. M.; Diken, E. G.; Roscioli, J. R.; Weddle, G. H.; Johnson, M. A. *Science* **2004**, *306*, 675–679.
(13) Roscioli, J. R.; Hammer, N. I.; Johnson, M. A.; Diri, K.; Jordan, K. D. *J. Chem. Phys.* **2008**, *128*, 104314.
(14) Shin, J.-W.; Hammer, N. I.; Headrick, J. M.; Johnson, M. A. *Chem. Phys. Lett.* **2004**, *399*, 349–353.
(15) Verlet, J. R. R.; Bragg, A. E.; Kammrath, A.; Cheshnovsky, O.; Neumark, D. M. *Science* **2005**, *307*, 93–96.
(16) Hammer, N. I.; Roscioli, J. R.; Johnson, M. A. *J. Phys. Chem. A* **2005**, *109*, 7896–7901.
(17) Nigra, P.; Carignano, M. A.; Kais, S. *J. Chem. Phys.* **2001**, *115*, 2621–2628.
(18) Maheshwary, S.; Patel, N.; Sathyamurthy, N.; Kulkarni, A. D.; Gadre, S. R. *J. Phys. Chem. A* **2001**, *105*, 10525–10537.
(19) Carignano, M. A. *Chem. Phys. Lett.* **2002**, *361*, 291–297.
(20) Serra, P.; Kais, S. *Chem. Phys. Lett.* **2003**, *372*, 205–209.
(21) Hammer, N. I.; Hinde, R. J.; Compton, R. N.; Diri, K.; Jordan, K. D.; Radisic, D.; Stokes, S. T.; Bowen, K. H. *J. Chem. Phys.* **2004**, *120*, 685–690.
(22) Lee, H. M.; Kim, K. S. *J. Chem. Phys.* **2002**, *117*, 706–708.
(23) Roscioli, J. R.; Johnson, M. A. *J. Chem. Phys.* **2007**, *126*, 024307.
(24) Berendsen, H. J. C.; van der Spoel, D.; van Drunen, R. *Comput. Phys. Commun.* **1995**, *91*, 43–56.
(25) Lindahl, E.; Hess, B.; van der Spoel, D. *J. Mol. Mod.* **2001**, *7*, 306–317.
(26) van der Spoel, D.; Lindahl, E.; Hess, B.; Groenhof, G.; Mark, A. E.; Berendsen, H. J. C. *J. Comput. Chem.* **2005**, *26*, 1701–1718.
(27) Berendsen, H. J. C.; Grigera, J. R.; Straatsma, T. P. *J. Phys. Chem.* **1987**, *91*, 6269–6271.
(28) Hukushima, K.; Nemoto, K. *J. Phys. Soc. Jpn.* **1996**, *65*, 1604–1608.
(29) Ryckaert, J. P.; Ciccotti, G.; Berendsen, H. J. C. *J. Comput. Phys.* **1977**, *23*, 327–341.
(30) Frisch, M. J.; Trucks, G. W.; Schlegel, H. B.; Scuseria, G. E.; Robb, M. A.; Cheeseman, J. R.; Montgomery, J. A., Jr.; Vreven, T.; Kudin, K. N.; Burant, J. C.; Millam, J. M.; Iyengar, S. S.; Tomasi, J.; Barone, V.; Mennucci, B.; Cossi, M.; Scalmani, G.; Rega, N.; Petersson, G. A.; Nakatsuji, H.; Hada, M.; Ehara, M.; Toyota, K.; Fukuda, R.; Hasegawa, J.; Ishida, M.; Nakajima, T.; Honda, Y.; Kitao, O.; Nakai, H.; Klene, M.; Li, X.; Knox, J. E.; Hratchian, H. P.; Cross, J. B.; Bakken, V.; Adamo, C.; Jaramillo, J.; Gomperts, R.; Stratmann, R. E.; Yazyev, O.; Austin, A. J.; Cammi, R.; Pomelli, C.; Ochterski, J. W.; Ayala, P. Y.; Morokuma, K.; Voth, G. A.; Salvador, P.; Dannenberg, J. J.; Zakrzewski, V. G.; Dapprich, S.; Daniels, A. D.; Strain, M. C.; Farkas, O.; Malick, D. K.; Rabuck, A. D.; Raghavachari, K.; Foresman, J. B.; Ortiz, J. V.; Cui, Q.; Baboul, A. G.; Clifford, S.; Cioslowski, J.; Stefanov, B. B.; Liu, G.; Liashenko, A.; Piskorz, P.; Komaromi, I.; Martin, R. L.; Fox, D. J.; Keith, T.; Al-Laham, M. A.; Peng, C. Y.; Nanayakkara, A.; Challacombe, M.; Gill, P. M. W.; Johnson, B.; Chen, W.; Wong, M. W.; Gonzalez, C.; Pople. J. A.; Gaussian, Inc.: Wallingford, CT, 2004.
(31) Wales, D. J.; Ohmine, I. *J. Chem. Phys.* **1993**, *98*, 7245–7256.
(32) Tsai, C. J.; Jordan, K. D. *J. Chem. Phys.* **1993**, *99*, 6957–6970.
(33) Egorov, A. V.; Brodskaya, E. N.; Laaksonen, A. *Mol. Phys.* **2002**, *100*, 941–951.
(34) Burnham, C. J.; Li, J.; Xantheas, S. S.; Leslie, M. *J. Chem. Phys.* **1999**, *110*, 4566–4581.
(35) Arbuckle, B. W.; Clancy, P. *J. Chem. Phys.* **2002**, *116*, 5090–5098.
(36) Herbert, J. M.; Head-Gordon, M. *J. Phys. Chem. A* **2005**, *109*, 5217–5229.

JP901047Y